 CMES, vol.104, no.2, pp.105-132, 2015

Turbulent Inlet Conditions Modeling using Large-eddy Simulations

M.M.R. Damasceno[1], J.M. Vedovoto[1] and A. da Silveira-Neto[1]

Abstract: Turbulence is a phenomenon which presents peculiarities when it is experimented or simulated. This occurs due to its complexity and high sensibility to the inlet conditions of the turbulent flow fields, as well as the presence of a large range of time and length scales. A simplification for this situation is obtained with the use of approximations and turbulence models. In the present work, the Large-eddy Simulations methodology was applied, aiming the modeling of the previously mentioned complexity, which consists in using a filter to resolve the large scales while the remaining scales were determined by classical and dynamic Smagorinsky models. Three different approximations for the inlet conditions were applied: white noise, Random Flow Generation (RFG) and Synthetic Eddy Method (SEM). It was possible to realize that the use of the dynamic Smagorinky model and the RFG or SEM methodologies resulted in a better characterization of the studied flow.

Keywords: turbulent inlet conditions, turbulence models, large-eddy simulations.

1 Introduction

The turbulence phenomenon is a flow regime characterized by presenting peculiarities on its numerical or material experimentation. This is due to its complexity and, also, sensibility to the turbulent flows initial and boundary conditions. It is defined by a wide range of time and length scales. The consequence is that a detailed description of such flows is normally very complex.

The application of the Navier-Stokes equations for modeling laminar or turbulent flows allows the characterization of these phenomena in a detailed and accurate way. This sensibility generates difficulties for turbulence prediction, because these equations describe all the velocity and pressure fields for all the scales of time and length, as well as their nonlinear interactions. It is a wide amount of information contained in these fields and, as consequence, the direct resolution of the related system of equations for practical situations becomes impossible. In this context,

[1] UFU, Uberlândia, MG, Brazil.

three main resolution methodologies can be applied: Direct Numerical Simulations (DNS), Large Eddy Simulations (LES) and Reynolds Averaged Navier-Stokes (RANS).

With the use of DNS methodology, all the turbulence scales are calculated using the Navier-Stokes equations without an additional turbulence model. As a consequence, a mesh refinement capable of picking up all the frequency spectrum, from the largest structures until the Kolmogorov scale, is required. Due to the large scales spectrum that appears in engineering situations, this methodology is hard to be applied. However, it is very powerful for a detailed description of low Reynolds number flows. Other methodologies appeared from the difficulty of using the DNS to solve high Reynolds number flows. In this context, the turbulence scales decomposition was proposed, using temporal averages or spatial filtrations.

The application of temporal averages results in a decomposition of the velocity into mean and floating parts. The application of this methodology, known as RANS, requires a complete modeling of the energy spectrum and, for this reason, very robust models become necessary in order to calculate the additional tensor, which appears due to the advective term of the Navier-Stokes equations, after the turbulence scales decomposition.

The use of spatial and temporal filters, by the other hand, produces the filtered Navier-Stokes equations, which are related to the LES methodology. The applied filter, that is associated to the discretization mesh and to the time step, has the role of separating the flow scales. This artifice allows the modeling of structures smaller than the mesh used and the calculation of the remaining ones.

The RANS methodology requires a lower refinement, when compared to DNS or LES. For this reason, it is applicable in high Reynolds flows. However, a significant amount of informations is lost because all the energy spectrum is modeled. In other words, the choice between the mentioned methodologies must be performed by the researcher, relying on what kind of analysis is intended to be done.

Mariano, Moreira, Silveira-Neto, da Silva, and Pereira (2010) developed a numerical methodology combining Fourier pseudo-spectral and immersed boundary methods, named IMERSPEC. Such a numerical tool was created for the characterization of fluid flows governed by the incompressible Navier-Stokes equations. With the use of the referred computational code, Moreira, Mariano, and Silveira-Neto (2011) showed the importance of turbulence modeling in the simulation of turbulent flows with the use of the LES methodology. For this purpose, a homogeneous isotropic turbulence in a periodic box was experimented by adding a body force to the Navier-Stokes equations. Such modification was realized in order to model the injection of energy at low wave numbers. An interesting result of this work was

the obtainment of a Smagorinsky's constant of $C_S = 0.18$ as been the best value for the characterization of the proposed phenomenon. This result is equivalent to what was obtained by Lilly (1967), in an analytical procedure.

Based on the aforementioned studies, the present work is intended to compare the use of two different turbulence models (Smagorinsky classical and dynamic models), as well as the application of different turbulent inlet conditions generation methods in a LES approach, implemented in a computational code based on the finite volumes methodology. The mathematical modeling for such approximations is presented as follows.

2 Mathematical modeling

In the present work, an approach based on the filtered Navier-Stokes equations was retained. This methodology separates the turbulent kinetic energy spectrum in two parts: the first, located before the cut-off frequency of the filter, which will be calculated, and the second, positioned after this frequency. The scales that compose this part of the spectrum are named sub-grid scales. The non linear energy transfer between these two parts of the spectrum is modeled using subgrid scales turbulence models. The large scales, responsible for the global characterization of the flow and the transport of most quantity of energy, are directly calculated, while the energy transfer is modeled.

Thereby, the variables present in the Navier-Stokes equations are separated in filtered, $\bar{f}(\vec{x},t)$, and float or sub-grid scales, $f'(\vec{x},t)$:

$$f(\vec{x},t) = \bar{f}(\vec{x},t) + f'(\vec{x},t), \tag{1}$$

where the filtered part is defined as:

$$\bar{f}(\vec{x},t) = \int_D f(\vec{x}',t) G(\vec{x}-\vec{x}') d\vec{x}'. \tag{2}$$

The filter function should be defined as a volumetric filter, for example:

$$G(\vec{x}) = \begin{cases} 1/\Delta^3 & \text{se } |\vec{x}| \leq \Delta/2 \\ 0 & \text{se } |\vec{x}| > \Delta/2 \end{cases}, \tag{3}$$

where Δ denotes the filter length and, as a consequence, the cut-off wave number.

The application of this scale decomposition, as well as of this filtering process, results in the Navier-Stokes filtered equations, as follows:

$$\frac{\partial \overline{u_i}}{\partial t} + \frac{\partial}{\partial x_j}(\overline{u_i}\,\overline{u_j}) = -\frac{1}{\rho}\frac{\partial \overline{p}}{\partial x_i} + \frac{\partial}{\partial x_j}\left[\nu\left(\frac{\partial \overline{u_i}}{\partial x_j} + \frac{\partial \overline{u_j}}{\partial x_i}\right) - (L_{ij} + \tau_{ij} + C_{ij})\right] \tag{4}$$

Thereby, the generated system of equations consists of four variables and four equations, coupled with three additional tensors (τ_{ij}, C_{ij} and L_{ij}). The addition of other transport equations, for modeling these tensors, would result in the appearance of higher order momentum, which is known as the turbulence closing problem. Such an indetermination can be treated with the application of the Boussinesq's hypothesis, which proposes the calculation of the sub-grid Reynolds' tensor τ_{ij} as being proportional to the strain rate generated by the filtered velocity field and the turbulent kinetic energy. In other words:

$$\tau_{ij} = -\nu_t \left(\frac{\partial \overline{u}_i}{\partial x_j} + \frac{\partial \overline{u}_j}{\partial x_i} \right) + \frac{2}{3} k \delta_{ij}, \tag{5}$$

where the turbulent viscosity ν_t is determined from closure models and the turbulent kinetic energy k is incorporated to the pressure gradient term.

Shaanan, Ferziger, and Reynolds (1975) and Silveira-Neto, Grand, Metais, and Lesieur (1993) showed that the Leonard's and cross tensors (L_{ij} and C_{ij}, respectively) are not required to be modeled in a separated way of the sub-grid Reynolds' stress tensors. Such a conclusion is due to the significant difference between the numerical values of these tensors when they are compared to the sub-grid Reynolds' stress tensor. Therefore, it is interesting to represent the filtered product $\overline{u_i u_j}$ by the global Germano's tensor [Germano, Piomelli, Moin, and Cabot (1991)]:

$$\tau_{ij} = \overline{u_i u_j} - \bar{u}_i \bar{u}_j. \tag{6}$$

It is interesting to emphasize that this global tensor incorporates all the aforementioned tensors: subgrid Reynolds tensor Leonard's and cross tensors.

Most sub-grid models are based on turbulent viscosity. Among them, the classical and dynamic Smagorinsky models are the most popular. Both were applied in the present work.

The classical sub-grid model, proposed by Smagorinsky (1963), for the determination of the turbulent viscosity is given by Eq. 7, in which C_s represents the Smagorinsky constant and Δ is the length-scale related to the filter (mesh spacing).

$$\nu_t = (C_S \Delta)^2 \sqrt{2 \overline{S}_{ij} \overline{S}_{ij}}. \tag{7}$$

The constant C_S must be adjusted, for each kind of flow, with numerical values normally between 0.05 and 0.30. For situations in which homogeneous and isotropic turbulence are modeled, Lilly (1967) determined $C_S = 0.18$, using an analytical procedure.

An important issue related to the application of this turbulence model is its lack of capability of performing precise calculations of the turbulent viscosity in parietal

regions. For this reason, the appliance of a damping function becomes necessary. In the present work, the van Driest damping function, proposed by van Driest (1956), was applied:

$$C_{SA} = C_S(1 - e^{-d^*/A^+})^2 z, \tag{8}$$

where $d^* = du_\tau/\nu$ denotes the distance from the wall, $u_\tau = \sqrt{\tau_w/\rho}$ is related to the shear velocity, τ_w corresponds to the shear stress close to the wall, $A^+ = 25$ is a constant determined by Ferziger and Perić (2002) and C_S is the Smagorinsky constant, previously mentioned.

The Smagorinsky dynamic model, proposed by Germano, Piomelli, Moin, and Cabot (1991), is based on a function capable of adjusting itself to the flow in time and space and in the application of two filters with different characteristic lengths. Thereby, this methodology is oriented by the informations of the energy levels contained in the smallest resolved scales, located between both filters, for modeling the energy transfer between the resolved and modeled scales. Both filtered Navier-Stokes equations are shown in Eq. 9 and Eq. 10:

$$\frac{\partial \overline{u}_i}{\partial t} + \frac{\partial}{\partial x_j}(\overline{u}_i \overline{u}_j) = -\frac{1}{\rho}\frac{\partial \overline{p}}{\partial x} + \frac{\partial}{\partial x_j}\left[\nu\left(\frac{\partial \overline{u}_i}{\partial x_j} + \frac{\partial \overline{u}_j}{\partial x_i}\right) - \tau_{ij}\right], \tag{9}$$

$$\frac{\partial \hat{\overline{u}}_i}{\partial t} + \frac{\partial}{\partial x_j}(\hat{\overline{u}}_i \hat{\overline{u}}_j) = -\frac{1}{\rho}\frac{\partial \hat{\overline{p}}}{\partial x} + \frac{\partial}{\partial x_j}\left[\nu\left(\frac{\partial \hat{\overline{u}}_i}{\partial x_j} + \frac{\partial \hat{\overline{u}}_j}{\partial x_i}\right) - T_{ij}\right]. \tag{10}$$

where $\tau_{ij} = \overline{u_i u_j} - \bar{u}_i \bar{u}_j$ denotes the Germano's global tensor and $T_{ij} = \widehat{\overline{u_i u_j}} - \hat{\bar{u}}_i \hat{\bar{u}}_j$ corresponds to the subtest tensor.

The determination of the function responsible for the generation of the dynamic coefficient of this proposition is obtained from the use of the Germano's identity, $L_{ij} = \widehat{\overline{u_i}\overline{u_j}} - \hat{\bar{u}}_i \hat{\bar{u}}_j = T_{ij} - \hat{\tau}_{ij}$, and $M_{ij} = \hat{\overline{\Delta}}^2 |\hat{\overline{S}}_{ij}| \hat{\overline{S}}_{ij} - \hat{a}$, where $\hat{a} = \overline{\Delta}^2 |\overline{S}_{ij}| \overline{S}_{ij}$. The function previously mentioned is presented as follows:

$$c(\vec{x}, t) = \frac{1}{2}\frac{L_{ij} M_{ij}}{M_{ij} M_{ij}}. \tag{11}$$

The capability of this function of adjusting itself to the flow in time and space is an important improvement. However, it is expected that better results can be achieved with the application of more realistic inlet conditions. In this context, two methodologies were studied in the present work: the Random Flow Generation (RFG), proposed by Smirnov, Shi, and Celik (2001) and the Synthetic Eddy Method (SEM), presented by Jarrin, Benhamadouche, Laurence, and Prosser (2006).

2.1 Random Flow Generation

The RFG is a modified version of the technique presented by Kraichnan (1970). It can be defined as orthogonal and scaling transformations applied to a continuous flow field, generated by a superposition of harmonic functions.

This methodology requires an anisotropic velocity correlation tensor

$$r_{ij} = \overline{\tilde{u}_i \tilde{u}_j} \tag{12}$$

and the determination of an orthogonal transformation tensor, a_{ij}, to diagonalize r_{ij}:

$$a_{mi} a_{nj} r_{ij} = \delta_{mn} c_n^2 \tag{13}$$

$$a_{ik} a_{kj} = \delta_{ij} \tag{14}$$

There by, a_{ij} and c_n becomes known functions in space. The variable c_n represents the velocity fluctuations in the new coordinates system, produced by the transformation tensor a_{ij}. Hereafter, a transient flow field is generated in a three dimensional domain using the Kraichnan's modified method:

$$v_i(\vec{x},t) = \sqrt{\frac{2}{N}} \sum_{n=1}^{N} [p_i^n cos(\tilde{k}_j^n \tilde{x}_j + \omega_n \tilde{t}) + q_i^n sen(\tilde{k}_j^n \tilde{x}_j + \omega_n \tilde{t})]. \tag{15}$$

Finally, orthogonal and scaling transformations are applied to the previously generated field v_i, in order to obtain a new field u_i:

$$\begin{aligned} w_i &= c_i v_i, \\ u_i &= a_{ik} w_k. \end{aligned} \tag{16}$$

This procedure results in a transient field $u_i(\vec{x},t)$ with correlation functions $\overline{u_i u_j}$ equivalent to r_{ij}. It is a divergence-free field for any situation involving homogeneous turbulence and, for non-homogeneous turbulence cases, it presents high convergence orders.

2.2 Synthetic Eddy Method

The Synthetic Eddy Method - SEM [Jarrin, Benhamadouche, Laurence, and Prosser (2006)], is based on the characterization of turbulence as a superposition of coherent structures. Thereby, these eddies should be generated at the domain inlet plane of the studied physical domain and defined by a function responsible for carrying the spatial and temporal characteristics of this phenomenon.

This methodology can be better explained from an unidimensional case, in which one unique velocity component will be generated on the interval $[a,b]$. The variable $f_\sigma(x)$ denotes a shape function of a turbulent spot, which presents a compact support on $[-\sigma,\sigma]$ and satisfies the normalization condition

$$\frac{1}{\Delta} = \int_{-\Delta/2}^{\Delta/2} f_\sigma^2(x)dx = 1, \tag{17}$$

where $\Delta = b-a+2\sigma$. Each turbulent spot has a position x_i, a length scale σ and receives a signal ε_i. Thus, the contribution $u_i(x)$ of a turbulent spot to the velocity field, is defined as:

$$u_i(x) = \varepsilon_i f_\sigma(x-x_i), \tag{18}$$

where ε_i represents a binary random variable, of value -1 or $+1$ and x_i is drawn randomly on the interval $[a-\sigma,b+\sigma]$. The synthetic eddies are generated on an interval larger than $[a,b]$, in order to guarantee that the boundary points can be surrounded by eddies. The velocity signal at any point is the sum of the contributions of all synthetic eddies on the domain:

$$u(x) = \frac{1}{\sqrt{N}}\sum_{i=1}^{N} \varepsilon_i f_\sigma(x-x_i), \tag{19}$$

in which N denotes the quantity of synthetic eddies.

For 2d situations, the eddies are now 3d structures with compact three-dimensional supports on $[-\sigma_x,\sigma_x;-\sigma_y,\sigma_y;-\sigma_z,\sigma_z]$, satisfying a three-dimensional normalization condition of the same type as presented in Eq. 17. The inlet plane is located at $x=0$ and it has dimensions $[0,L_z]\times[0,L_y]$. The position (x_i,y_i,z_i) of a synthetic eddy i is drawn randomly on $[-\sigma_x,\sigma_x]\times[-\sigma_y,L_y+\sigma_y]\times[-\sigma_z,L_z+\sigma_z]$. The eddies are convected through the inlet plane with a reference velocity scale U_0, using Taylor's frozen turbulence hypothesis:

$$x_i(t+dt) = x_i(t)+U_0 dt \tag{20}$$

In case $x_i(t) > \sigma_x$, the synthetic eddie will be reallocated at $x=-\sigma_x$, in order to be convected again. Thus, the synthetic velocity signal is defined as:

$$u'_j(x,t) = \frac{1}{\sqrt{N}}\sum_{i=1}^{N} \varepsilon_{ij} f_j(x-x_i(t)), \tag{21}$$

in which ε_{ij} denotes the sign of vortex i on component j and are independent random steps of values -1 or $+1$.

The independence of ε_{ij} ensures that the generated inflow signal satisfies the condition $\overline{u_i u_j} = \delta_{ij}$. Thus, the availability of the Reynolds' stress tensor, R_{ij} and of the mean velocity profile, $\bar{u}_i$, obtained from previous experiments, allows the transformation of the generated signal, in order to perform a more accurate characterization [Lund, Wu, and Squires (1998)]. The final velocity field u_i is, therefore, reconstructed from a synthetic field u'_i, a mean velocity profile and a Cholesky's decomposition, obtained from the provided Reynolds' stress tensor:

$$u_i = \bar{u}_i + a_{ij} u'_j, \tag{22}$$

in which a_{ij} is related to the Cholesky's decomposition:

$$\mathbf{a_{ij}} = \begin{pmatrix} \sqrt{R_{11}} & 0 & 0 \\ R_{21}/a_{11} & \sqrt{R_{22} - a_{21}^2} & 0 \\ R_{31}/a_{11} & (R_{32} - a_{21}a_{31})/a_{22} & \sqrt{R_{33} - a_{31}^2 - a_{32}^2} \end{pmatrix}. \tag{23}$$

3 Results

The computational code used in the present work, named Fluids3D, was developed by Vedovoto, Silveira-Neto, Mura, and Silva (2011), is based on the finite volumes method, composed by staggered variables three dimensional fields and is, also, conservative. A centered differences scheme is applied for denoting the diffusive and advective contributions of the transport equations and a fully implicit approximation is adopted. The resultant linear system is solved using the MSIP - Modified Strongly Implicit Procedure [Schneider and Zedan (1981)] for the velocity components. The mesh is cartesian, structured and uniform.

This computational code adopts an approximation based on the pressure, as a consequence, an algorithm for the pressure-velocity coupling becomes necessary. Thereby, a projection method based on the fractional steps technique is applied, resulting in a Poisson's equation composed by variable coefficients, which is resolved with the solver BICGSTAB - Bi-Conjugate Gradient Stabilized [van der Vorst (1981) and Norris (2001)].

Such numerical tool was used, in the present work, to analyze two distinct experiments: a low-Reynolds flow occurring on a backward-facing step (computational code validation) and a study of the influence of different turbulence models and inlet conditions in a high-Reynolds flow characterization. These situations were simulated and the obtained results were compared with published references.

3.1 Validation of the Computational Code Fluids 3D

Lee and Mateescu (1998) performed some experimentations of flows occurring on

a backward-facing step. These experiments were based on distinct sudden expansions, created by controlling the domain inlet step height, H. A schematic illustration of such experiment is shown in Fig. 1:

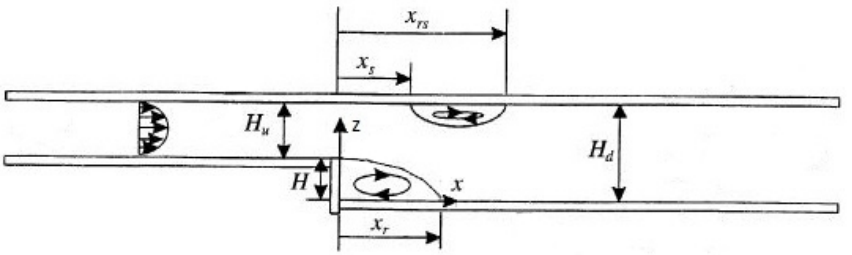

Figure 1: Schematic illustration of the experiment realized by Lee and Mateescu (1998).

The validation of the computational code used was performed with numerical simulations of one situation studied by Lee and Mateescu (1998). The calculations were realized in only one computer, composed by a Intel i5-750 CPU running at 2.67 GHz, with four processing cores and 4 Gb of RAM memory.

The results achieved were compared with the experiment realized by Lee and Mateescu (1998) and with the numerical simulations performed by Mariano (2011). The last reference presented simulations of the studied experiment realized in another computational code, named IMERSPEC [Mariano, Moreira, Silveira-Neto, da Silva, and Pereira (2010)], which is based on a spectral methodology for resolving the differential equations which characterize the studied situation.

The simulated experiment was composed by a domain length $L = 34.44\ m$, a domain height $H_d = 1.0\ m$ and a step height $H = 0.5\ m$. This flow experiments a Reynolds number $Re = 400$ and its inlet mean velocity profile is defined as:

$$u(z) = \begin{cases} -24(H_d - z)(H - z) & \text{if} \quad H < z \leq H_d, \\ 0 & \text{if} \quad 0 \leq z \leq H, \end{cases} \tag{24}$$

in which an advective boundary condition was applied at the end of the domain and a no slip condition was applied into the inferior and superior limits of the domain in z-direction, aiming to achieve the no-slipping boundary condition.

Three different mesh refinements were used (1024x32, 2048x64 e 4096x128 volumes), without the appliance of turbulence models. The obtained results were related to a time period of 400 physical seconds. The mean velocity profiles obtained in the present work, evaluated in vertical stations located at $x = 7\ m$ and $x = 14\ m$ of

the domain, are presented in Fig. 2. The analysis of the aforementioned figure suggests a good accordance between the results achieved in the present work and the experimentation performed by Lee and Mateescu (1998) and, also, the calculations realized by Mariano (2011).

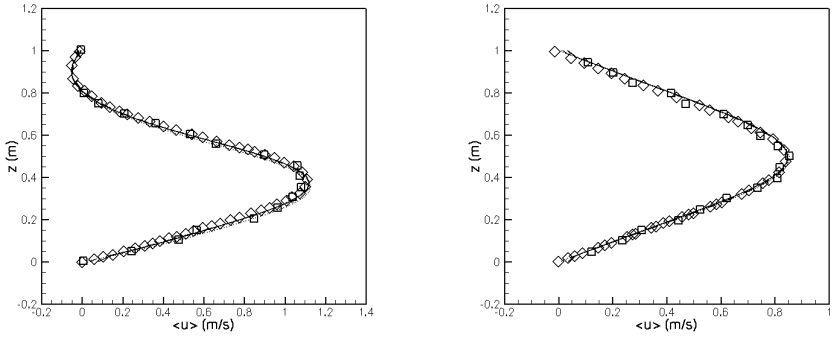

(a) (b)

Figure 2: Mean velocity situated at the following vertical stations: (a) $x = 7m$ and (b) $x = 14m$.
□ Lee and Mateescu (1998) ♢ Mariano (2011) — present work (1024x32) - - - present work (2048x64) ⋯ present work (4096x128)

One interesting analysis, when backward-facing steps are observed, is the comparison between the recirculation lengths generated due to the sudden expansion. In the present work, the distances between the sudden expansion beginning and the inferior and superior recirculations end are defined as x_r and x_{rs}, x_s is related to the distance between the beginnings of the sudden expansion and the superior recirculation. In this context, the Tab. 1 shows data related the aforementioned lengths, obtained from the numerical simulations performed in the present work and in the calculations realized by Mariano (2011). These results were determined by the analysis of the flow stream lines. The relative deviations of these results, when compared with the experimental data obtained by Lee and Mateescu (1998) are also presented.

The analysis of the obtained data suggests that, since the second mesh refinement, the recirculation lengths become quite close to the results determined experimentally and numerically, which guarantees the validation of the developed computational code. The mesh independence is also observed starting from the second mesh refinement. Such an independence is observed due to the insignificant changes on results with the mesh refinement increase.

Table 1: Characteristic recirculation lengths in a backward-facing step flow.

Work	x_r/H	Deviance	x_s/H	Deviance	x_{rs}/H	Deviance
Lee and Mateescu (1998)	12.90	—	10.30	—	20.5	—
Mariano (2011) - 4096x128	12.19	5.5%	9.94	3.5%	20.7	0.97%
Present work - 1024x32	12.05	6.59%	9.6	6.80%	20.2	1.46%
Present work - 2048x64	12.3	4.65%	9.8	4.85%	20.65	0.73%
Present work - 4096x128	12.25	5.04%	9.8	4.85%	20.7	0.97%

Another analysis was performed, in order to compare both differential equations resolution methodologies (finite volumes and spectral methods): the processing time required to conclude the aforementioned simulations. For this purpose, the calculations were realized in a single CPU, presenting almost the same characteristics (except the differential equations resolution methodology). The analysis was performed by a performance evaluation of the computational codes FLUIDS 3D (based on finite volumes) and IMERSPEC (implemented with Fourier pseudo-spectral method) developed, respectively, by Vedovoto, Silveira-Neto, Mura, and Silva (2011) and Mariano (2011). The results are shown in Tab. 2 and Fig. 3.

A significant difference is observed between the processing time required by both codes. FLUIDS3D required a smallest quantity of computational time to perform similar calculations. However, it is important to mention that the IMERSPEC code presents high accuracy against the code based on finite volumes.

The validation of FLUIDS 3D allowed the realization of numerical simulations of more complex flows. As follows, results related to simulations of turbulent nonreactive flows occurring inside a combustion chamber will be presented.

Table 2: Amount of iterations and time required for the proposed calculations.

Mesh refinement	Computational code	Amount of iterations	Processing time (h)
1024x32	FLUIDS3D	23910	1.044
	IMERSPEC	22400	3.009
2048x64	FLUIDS3D	47940	6.19
	IMERSPEC	44800	28.2
4096x128	FLUIDS3D	95960	44.11
	IMERSPEC	89600	264.68

3.2 Turbulence modeling

Moreau, Tanguy, Gicquel, Poirot, and Sauzin (1996) performed experiments with

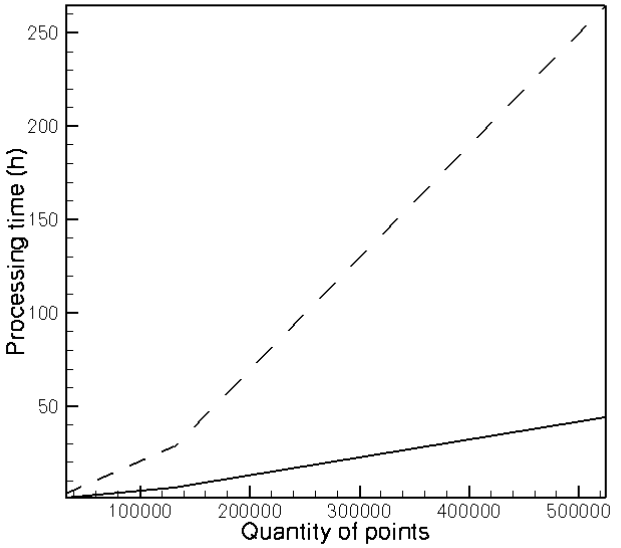

Figure 3: Processing time required by the studied computational codes.
— Fluids 3D - - - Imerspec

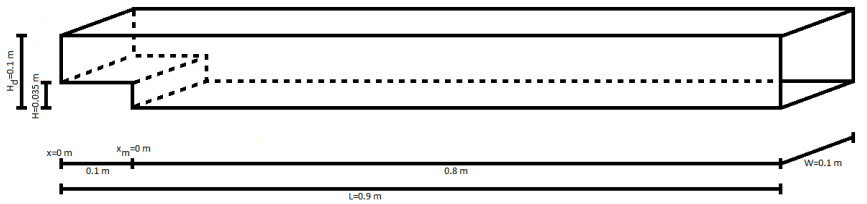

Figure 4: Schematic illustration of the experiment performed by Moreau, Tanguy, Gicquel, Poirot, and Sauzin (1996).

and without reactions in a combustion chamber, called A3C. A schematic figure of the used experimental stand is shown in Fig. 4. The data related to the longitudinal mean velocity fields $\bar{u}$ and its rms fluctuations u'_{rms} were taken, by the mentioned authors, using laser velocimetry.

The main characteristics of this experiment were the following: its length, height and width were, respectively, $L = 0.9\ m$, $H_d = 0.1\ m$ and $W = 0.1\ m$. The backward-facing step was composed by the following height, length and width: $H = 0.035\ m$,

$z_H = 0.1\ m$ and the same width of the chamber. The flow experimented $Re = 48750$ and the inlet mean velocity profile, fitted from the experimental data, was given by:

$$u(z) = \begin{cases} \overline{U}\left\{1 - \left[\dfrac{z - \left(\dfrac{H_u}{2} + H\right)}{\dfrac{H_u}{2}}\right]^{\psi}\right\} & \text{if} \quad H < z \leq H_d \\ 0 & \text{if} \quad 0 \leq z \leq H, \end{cases} \tag{25}$$

where $\overline{U} = 55\ m/s$, $H_u = 0.065\ m$, $\psi = 10$ and $H = 0.035\ m$.

Since the studied situation was a turbulent flow, its calculations required larger amounts of computational resources. For this reason, the simulations were performed in a SGI Altix XE 1300 system. It consisted of a cluster composed by 30 computational nodes, in which four of them were composed by two Intel Xeon E5540 processors, running at 2.53 GHz and 16 processing cores. The remaining nodes had two processors Intel Xeon E5650, running at 2.67 GHz and 24 processing cores. This computational infrastructure resulted in 688 processing cores, interconnected by an Infiniband QDR net. With this equipment, it was possible to perform numerical simulations of the mentioned experiment, using two different turbulence models and three distinct turbulent inlet generation methods. A brief description of the experiments realized in the present work is presented in Tab. 3:

Table 3: Numerical simulations performed in the present work.

Mesh refinement	Quantity of processors	Turbulence model	Inlet conditions generation method
450x50x50	80	Smagorinsky	White noise
450x50x50	80	Dynamic	White noise
450x50x50	100	Dynamic	Random Flow Generation (1000 Fourier modes)
450x50x50	36	Dynamic	Synthetic Eddy Method (10000 eddies)
450x50x50	100	Dynamic	Synthetic Eddy Method (100000 eddies)

At first, it was performed a comparison between two different 3D simulations of the mentioned situation: the use of the classical turbulence model, proposed by Smagorinsky (1963), with $C_S = 0,18$, and the use of the Smagorinsky dynamic model, proposed by Germano, Piomelli, Moin, and Cabot (1991). The obtained

results were compared to the experimental data of Moreau, Tanguy, Gicquel, Poirot, and Sauzin (1996).

Both simulations were performed using 80 processors, with a mesh refinement of 450x50x50 volumes. When the Smagorinsky classical model was applied, the calculations were realized until a time of 3.55 physical seconds, which required 322,800 iterations. It was necessary 233.54 hours of computational time to finish this numerical simulation. The application of the Smagorinsky dynamic model required different conditions. The calculations were performed until the simulation achieved 4.82 physical seconds, which required 447,740 iterations. In this case, it was required 318.48 hours to complete the numerical simulation.

The achieved results are presented in Fig. 5, which shows the mean velocity profiles determined in the present work and the experimental data obtained by Moreau, Tanguy, Gicquel, Poirot, and Sauzin (1996).

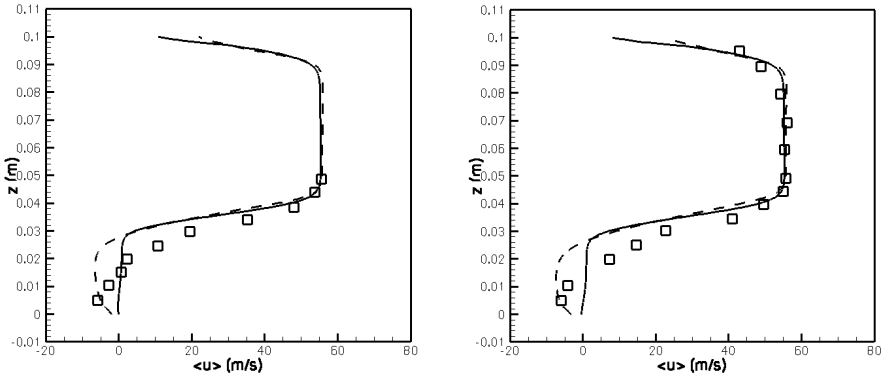

(a) (b)

Figure 5: Mean velocity profiles obtained from the application of the Smagorinsky classical and dynamic models: (a) $x_m = 0.08m$ and (b) $x_m = 0.10m$.
□ Moreau, Tanguy, Gicquel, Poirot, and Sauzin (1996) — Smagorinsky classical model - - - Smagorinsky dynamic model

The mean velocity profiles were better represented when the Smagorinsky dynamic model was applied. This affirmation can be proven by the analysis of the flow occurring close to the inferior wall. After that position, it is noticeable that this approximation was capable of following the tendency of the data obtained by Moreau, Tanguy, Gicquel, Poirot, and Sauzin (1996). However, the calculated values were far from the experimental data achieved by the adopted reference.

The results related to the mean velocity fluctuations, presented in Fig. 6, suggest

that a better fit to the experimental data was also achieved when the approximation proposed by Germano, Piomelli, Moin, and Cabot (1991) was used. The use of a function for the dynamic sub-grid scale turbulence model, which fits to the flow in time and space instead of a constant, as performed when the Smagorinky's classical model is used, is the main reason to what was presented before. However, there is still a noticeable deviance between the numerical results and the experimental data.

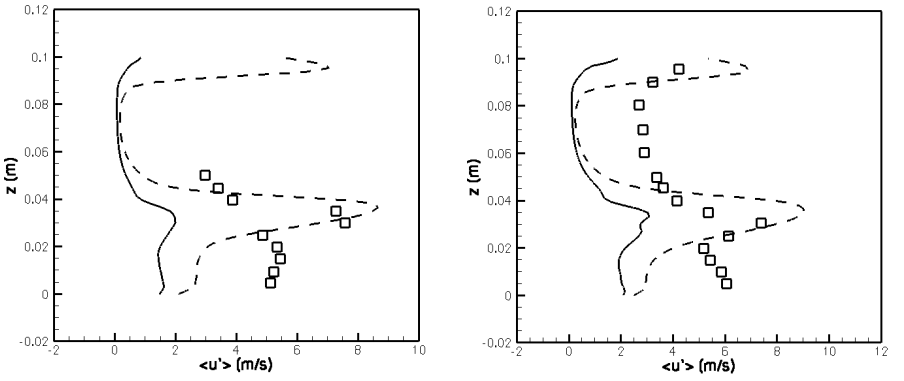

(a) (b)

Figure 6: Mean velocity fluctuations, obtained from the application of the Smagorinsky classical and dynamic models: (a) $x_m = 0.08m$ and (b) $x_m = 0.10m$. □ Moreau, Tanguy, Gicquel, Poirot, and Sauzin (1996) — Smagorinsky classical model - - - Smagorinsky dynamic model

The significant difference between the calculated results and the experimental data boosted us to study and apply more realistic inlet conditions to the numerical simulations, aiming the investigation of the influence of them on the studied flow.

Therefore, two distinct turbulent inlet conditions generation methods were applied to the following numerical simulations. At first, the methodology proposed by Smirnov, Shi, and Celik (2001), named Random Flow Generation, was applied. It consists of Fourier decompositions with coefficients calculated from spectral data obtained in different positions along the domain. Then, the approximation named Synthetic Eddy Method, proposed by Jarrin, Benhamadouche, Laurence, and Prosser (2006) was used. It is based on the creation of a box of eddies at the domain inlet.

The application of the RFG methodology on the studied problem was performed with 100 processors with a mesh refinement of 450x50x50 volumes. The calculations were realized until a time of 7.45 physical seconds, which required 502,180 iterations. It was necessary 166.12 hours of computational time to conclude this

simulation.

In Fig. 7 it is possible to observe a better fitting when the calculated mean velocity profiles are compared with the experimental data obtained by the adopted reference. This statement can be evaluated by observing a more accurate characterization of this flow in regions closer to the inferior wall.

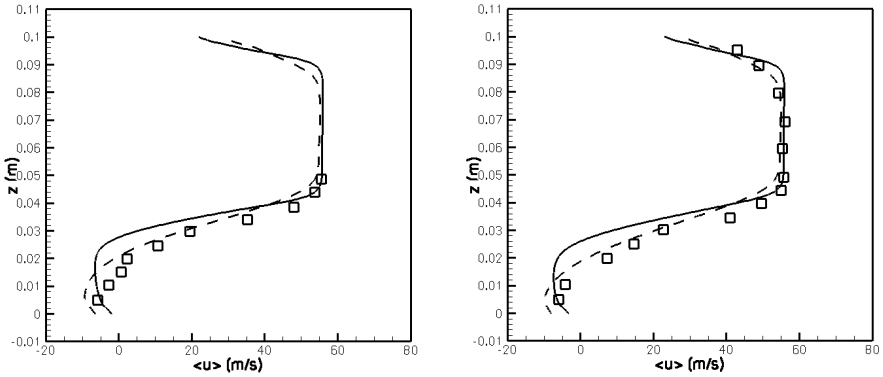

(a) (b)

Figure 7: Mean velocity profiles obtained from the application of the Smagorinsky dynamic model and the RFG method for the inlet turbulent conditions: (a) $x_m = 0.08\ m$ and (b) $x_m = 0.10\ m$.
□ Moreau, Tanguy, Gicquel, Poirot, and Sauzin (1996) — Smagorinsky dynamic model - - - Smagorinsky dynamic model with RFG.

The analysis of the mean velocity fluctuations profiles, presented by Fig. 8, suggests a significant improvement to the quality of the obtained results, when these are compared to the adopted reference. It is noteworthy that the results obtained in the present work behave similarly to the experimental data and these are more consistent in regions further from the sudden expansion.

After concluding the calculations presented before, studies concerning the methodology proposed by Jarrin, Benhamadouche, Laurence, and Prosser (2006) were performed. The Synthetic Eddy Method was firstly implemented in a computational code dedicated to evaluate its performance. Such a numerical code uses Reynolds' stress tensors experimental data and a mean velocity profile, along with the mentioned method, in order to create a turbulent velocity field at the domain inlet.

This methodology depends on the local turbulence characteristic length which is

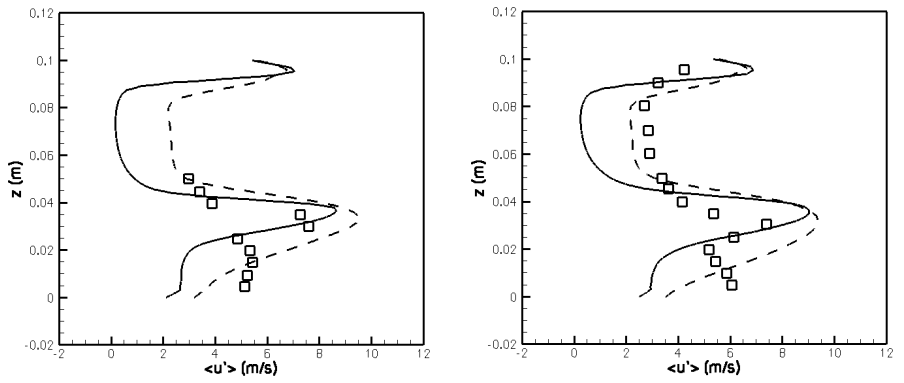

(a) (b)

Figure 8: Mean velocity fluctuations obtained from the application of the Smagorinsky dynamic model and the RFG method for the inlet turbulent conditions: (a) $x_m = 0.08m$ and (b) $x_m = 0.10m$.
□ Moreau, Tanguy, Gicquel, Poirot, and Sauzin (1996) — Dynamic Smagorinsky model - - - Dynamic Smagorinsky model with RFG.

determined, according to Pope (2000), using Eq. 26:

$$L = \frac{k^{3/2}}{\varepsilon}, \tag{26}$$

where $k = \dfrac{\overline{u'^2} + \overline{v'^2} + \overline{w'^2}}{2}$

However, it is well known that it is hard to obtain data representing the dissipation rate of a flow, which complicates the determination of the necessary characteristic length. For this reason, some attempts were realized and studied using the computational code mentioned earlier.

The influence of both number of eddies applied and performed iterations was evaluated from a set of numerical simulations, with 10,000 and 100,000 iterations with six different quantities of eddies and a constant time step of 0.000036 s. These evaluations were based on a comparison between the Reynolds' stress tensors experimented by the adopted reference and the results obtained in the present work.

At first, a characteristic length with a constant value of $L = 0.035$ m was used. The proposed simulations are presented in Tab. 4.

The other set of simulations was based on a proposition performed by Pope (2000), in which the dissipation rate was equivalent to the product between the kinematic

Table 4: Numerical simulations performed in order to evaluate the Synthetic Eddy Method, using a constant characteristic length.

Case	Iterations	Number of eddies	Characteristic length
A	10,000	100 500 1000 2000 10000 50000	$L = 0.035\ m$
B	100,000	100 500 1000 2000 10000 50000	

viscosity and the strain rate, as defined by Eq. 27:

$$\varepsilon \equiv 2\nu S_{ij} S_{ij}. \tag{27}$$

It was possible to determine the dissipation rate from the kinematic viscosity, mean velocity and step height, all obtained from the studied flow. This formulation is presented by Eq. 28:

$$\varepsilon = 2\nu \left(\frac{\partial \overline{u}_i}{\partial x_j}\right)\left(\frac{\partial \overline{u}_i}{\partial x_j}\right) \approx 2\nu \frac{\overline{U}^2}{H^2}. \tag{28}$$

As the dissipation rate was obtained, it was possible to realize the proposed simulations, which are shown in Tab. 5:

The obtained R_{11} Reynolds' stress tensor components were compared with the experimental data by the L_2 norm (Eq. 29). The achieved results are presented in Tab. 6 and Fig. 9.

$$L_2 = \sqrt{\frac{1}{N}\sum_{i=1}^{N}(R_{11_{calc}}^{(i)} - R_{11_{exp}}^{(i)})^2}, \tag{29}$$

where N denotes the quantity of points in the domain.

It is noteworthy that there is a significant variance between the L_2 norm values, according to the quantity of generated eddies. The best results were achieved when

Table 5: Numerical simulations performed in order to evaluate the Synthetic Eddy Method, using a characteristic length calculated using Eq. 26 and Eq. 28.

Case	Iterations	Number of eddies	Characteristic length
C	10,000	100 500 1000 2000 10000 50000	$L = \frac{k^{3/2}}{\varepsilon}, \varepsilon \approx 2\nu\frac{\overline{U}^2}{H^2}$
D	100,000	100 500 1000 2000 10000 50000	

the cases B and D were simulated, in this situations, a larger quantity of iterations was used. In the aforementioned cases it is also perceptible that the increase of the quantity of eddies resulted in better values of the analyzed norm.

The influence of the quantity of generated eddies and the characteristic length determination proposition in the CPU time required by the proposed methodology is presented in Tab. 7 and Fig. 10.

It is possible to note that increasing the quantity of generated eddies in this methodology, results in a linear increase of required computational time. As expected, the cases with larger amount of iterations (B and D) required more computational resources. At last, it is worth to note that the application of the first proposition, which was based on the application of a constant characteristic length, was the most expensive among the studied cases, while the use of the second proposition, based on Eq. 27, required less computational resources.

The results obtained with the appliance of the Synthetic Eddy Method were very promising, presenting turbulent kinetic energy distributed in a $-5/3$ scope along the flow frequencies, when this variable spectrum is evaluated. For this reason, this methodology was implemented in the FLUIDS 3D code, developed by Vedovoto, Silveira-Neto, Mura, and Silva (2011) and it was used to characterize the flow experimented by Moreau, Tanguy, Gicquel, Poirot, and Sauzin (1996). For this purpose, four numerical simulations were performed.

At first, the study of the influence of the quantity of generated eddies in the determi-

Table 6: L_2 norm obtained by the comparison between the Reynolds' stress tensors experimented by the adopted reference and calculated in the present work, using the Synthetic Eddy Method.

Quantity of eddies	L_2 Norm			
	A	B	C	D
100	3.84	0.79	4.52	1.44
500	2.97	0.33	4.18	1.69
1000	1.10	0.37	4.05	0.91
2000	1.14	0.69	5.65	2.15
10000	1.36	0.78	2.12	1.77
50000	2.27	0.57	2.64	1.20

Table 7: CPU time obtained with the application of the turbulent inlet boundary conditions generation method proposed by Jarrin, Benhamadouche, Laurence, and Prosser (2006).

Quantity of eddies	Processing time (s)			
	A	B	C	D
100	1.19	11.80	1.11	11.00
500	2.5	26.34	2.16	21.39
1000	4.11	43.81	3.47	34.46
2000	7.41	77.38	6.08	60.70
10000	33.52	353.25	26.80	265.14
50000	164.03	1774.21	131.31	1378.04

nation of the mean velocity and fluctuation profiles was performed. This analysis was done with two different numerical simulations. In the first simulation, 10,000 eddies were generated and 36 processors were used with a mesh refinement of 450x50x50 volumes. The calculations were performed until a time of 1.22 physical seconds, which required 87,180 iterations. It was necessary 71.88 hours of computational time to finish this requirements. In the second one, by the other hand, 100,000 eddies were generated and 100 processors were used with the same mesh refinement. The calculations were performed until a time of 2.20 physical seconds, which required 155,360 iterations. It was necessary 94.51 hours of computational time to finish this requirements. The achieved results are shown in Fig. 11 and Fig. 12.

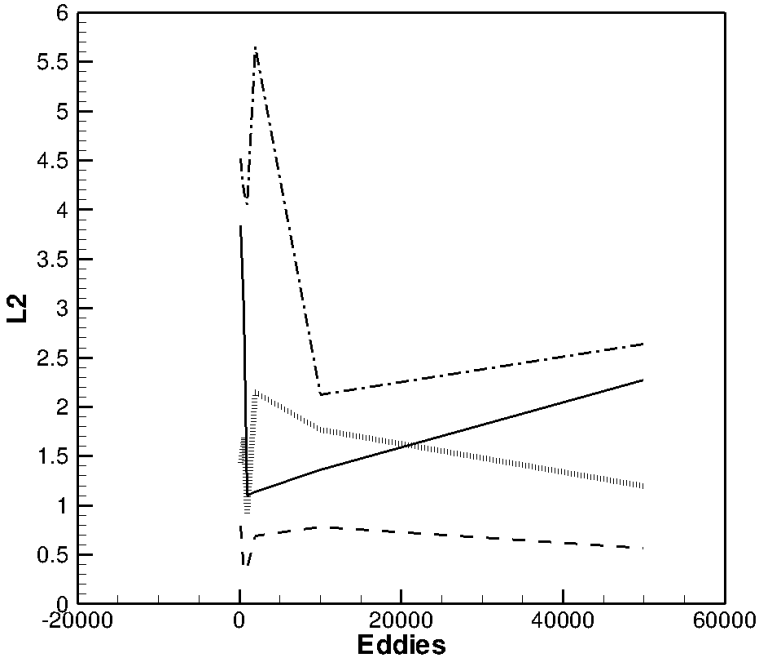

Figure 9: Influence of both quantity of generated eddies and characteristic length determination in the processing time required by the proposed methodology.
— case A - - - case B - · - case C ||| case D

From the analysis of the mean velocity profiles, presented by Fig. 11, it is possible to observe that there is no difference between the application of 10,000 or 100,000 eddies. A larger amount of eddies is responsible for an improvement to what was obtained when the RFG method was used.

From the evaluation of the mean velocity fluctuation profiles, presented in Fig. 12, it is possible to reinforce what was commented over the last paragraph. A larger amount of generated eddies was also responsible for a better characterization of the studied flow. For this reason, the situation in which the larger amount of generated eddies is used was applied to the last numerical simulations performed, which differ solely in the characteristic length calculation methodology.

The simulation in which the calculation of the characteristic length was performed via Eq. 27, required 114.4 hours of computational time for the numerical simulation

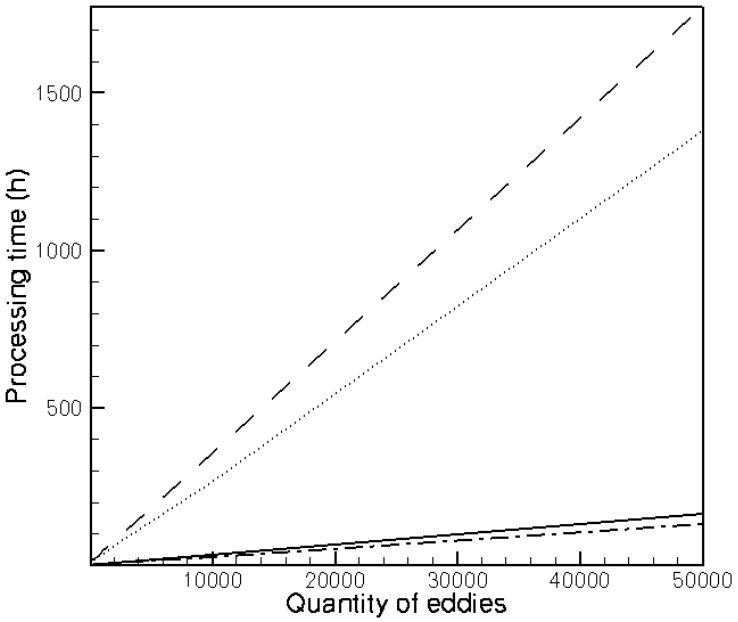

Figure 10: Influence of the quantity of generated eddies and the characteristic length determination proposition in the processing time required by the proposed methodology.
— case A - - - case B - · - case C ··· case D

of 2.14 physical seconds and 151,570 iterations. When a constant characteristic length was applied, 167.7 hours were needed to perform 350,880 iterations and 4.95 physical seconds. The mean velocity and mean velocity fluctuation profiles are shown in Fig. 13 and Fig. 14.

The analysis of the presented mean velocity profiles is sufficient to observe that the appliance of a constant characteristic length was capable to generate a better description of the flow, when a comparison with the other results is performed.

From the evaluation of the mean velocity fluctuations, it is noteworthy that, among the application propositions of the SEM, the use of Eq. 26 and Eq. 28 was the methodology which resulted in a better characterization of the studied flow. However, the best description was obtained using the methodology proposed by Smirnov, Shi, and Celik (2001).

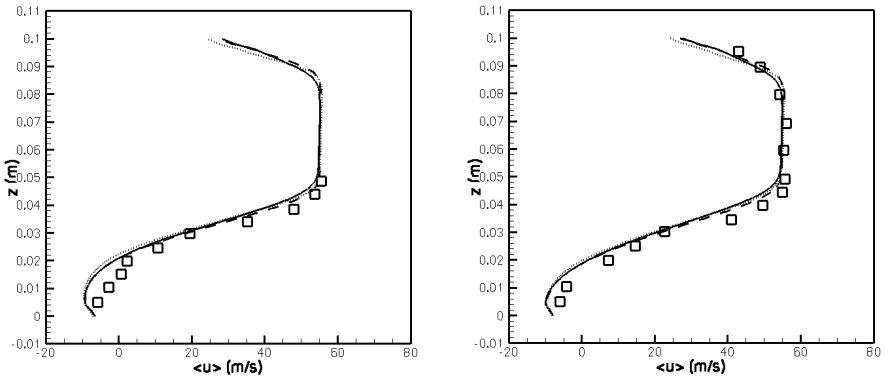

(a) (b)

Figure 11: Mean velocity profiles obtained from the application of the Smagorinsky dynamic model and the use of SEM and RFG methods for the turbulent inlet conditions: (a) $x_m = 0.08m$ and (b) $x_m = 0.10m$.
□ Moreau, Tanguy, Gicquel, Poirot, and Sauzin (1996) — RFG - - - SEM (10,000 eddies) - · - SEM (100,000 eddies)

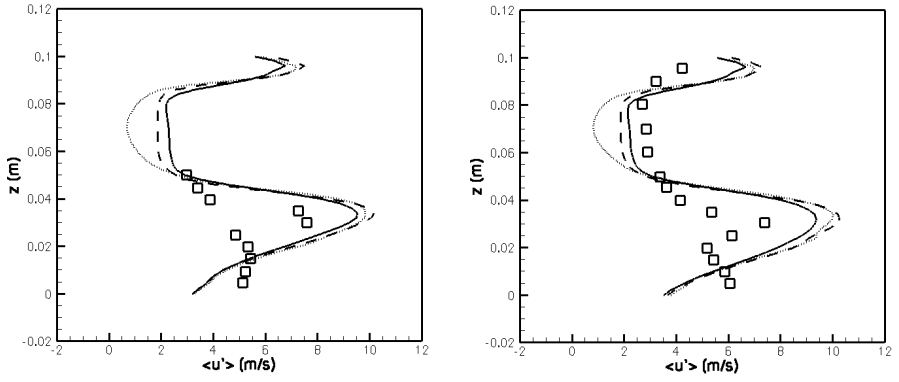

(a) (b)

Figure 12: Mean velocity fluctuations obtained from the application of the Smagorinsky dynamic model and the use of SEM and RFG methods for the inlet turbulent conditions: (a) $x_m = 0.08m$ and (b) $x_m = 0.10m$.
□ Moreau, Tanguy, Gicquel, Poirot, and Sauzin (1996) — RFG - - - SEM (10,000 eddies) - · - SEM (100,000 eddies)

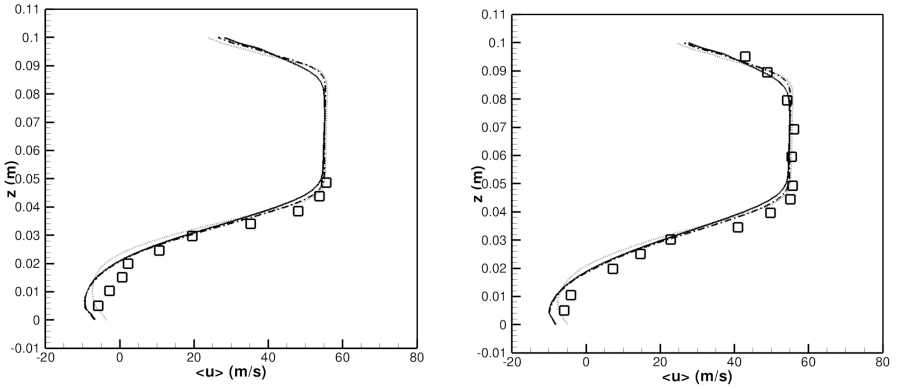

(a) (b)

Figure 13: Mean velocity profiles obtained from the application of the Smagorinsky dynamic model and the use of SEM and RFG methods for the turbulent inlet conditions: (a) $x_m = 0.08m$ and (b) $x_m = 0.10m$.
□ Moreau, Tanguy, Gicquel, Poirot, and Sauzin (1996) — RFG ··· SEM (case B) - · - SEM (case D)

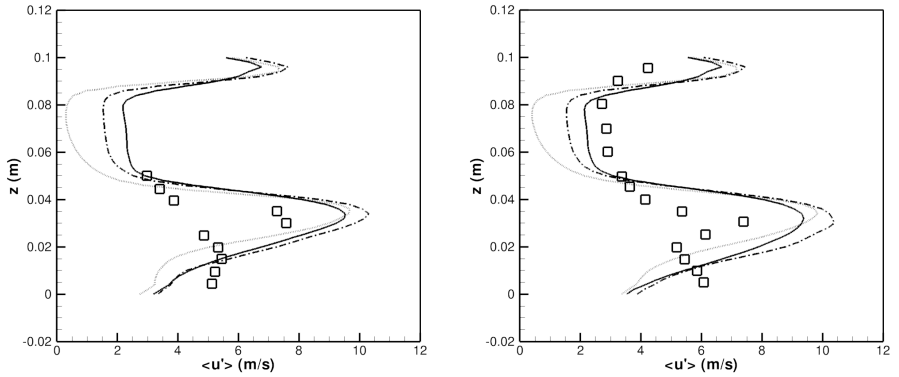

(a) (b)

Figure 14: Mean velocity fluctuations obtained from the application of the Smagorinsky dynamic model and the use of SEM and RFG methods for the inlet turbulent conditions: (a) $x_m = 0.08m$ and (b) $x_m = 0.10m$.
□ Moreau, Tanguy, Gicquel, Poirot, and Sauzin (1996) — RFG ··· SEM (case B) - · - SEM (case D)

A comparison between the computational costs required by both turbulent inlet conditions generators is shown in Tab. 8.

Table 8: Computational cost required by the turbulent inlet conditions proposed by Smirnov, Shi, and Celik (2001) and Jarrin, Benhamadouche, Laurence, and Prosser (2006).

Inlet conditions generation method	Physical time simulated (s)	Processing time (h)	Quantity of Iterations
Random Flow Generation	2.10	67.05	141,820
Synthetic Eddy Method - case 1		64.95	149,060
Synthetic Eddy Method - case 2		112.48	148,550

From the analysis of this table, it is worth to observe that, when an equal amount of physical time simulated is analyzed, the application of a constant characteristic length with the methodology proposed by Jarrin, Benhamadouche, Laurence, and Prosser (2006) was the simulation which required the less computational resources. The method proposed by Smirnov, Shi, and Celik (2001) needed the least quantity of iterations to achieve the same goal. Finally, the appliance of Eq. 26 and Eq. 27 for the determination of the characteristic length in SEM required a larger amount of computational time and iterations to perform the proposed calculations.

Conclusions

The realization of this work was motivated to study the influence of turbulent inlet boundary conditions in numerical simulations of flows in the context of large-eddy simulations.

The aforementioned studies were performed with a computational code developed by Vedovoto, Silveira-Neto, Mura, and Silva (2011), which was validated by comparisons with an experiment realized by Lee and Mateescu (1998) and numerical simulations, of the same problem, performed by Mariano (2011). In the meantime, the processing time required by both codes (FLUIDS3D and IMERSPEC) was evaluated. It was noteworthy that the Fluids 3D code, based on the finite volumes technique, required less computational resources to perform the same calculations.

After validating the aforementioned computational code, numerical simulations involving combinations of turbulence modeling and turbulent inlet conditions generation methods were realized. The obtained results were compared with experiments performed by Moreau, Tanguy, Gicquel, Poirot, and Sauzin (1996). These experiments denoted a turbulent flow occurring inside a combustion chamber.

At first, the appliance of the classical and dynamic Smagorinky's turbulence model was compared. From the analysis of these simulations, it was possible to realize that the dynamic Smagorinky's turbulence model gave a better flow characterization, when compared with the classical model. The presence of a function capable of self-adapting, instead of the Smagorinsky model, to simulate the flow in time and space was the main motive for this improvement.

The application of more realistic turbulent inlet conditions generation methods resulted in even better results, mainly when the mean velocity fluctuation profiles were analyzed. This fact is due to a better distribution of the turbulent kinetic energy, presenting the larger amount of energy in possession of the larger eddies.

Interesting results were obtained with the application of the Synthetic Eddy Method. This methodology achieved the best flow description when the mean velocities were analyzed. However, the mean velocity fluctuation profiles were better characterized by Random Flow Generation method.

From an exclusive analysis of the results obtained with the application of the SEM, it is noticeable that the use of a larger amount of eddies resulted in a better characterization of the mean velocity fluctuation profiles. It was observed, also, that the hypothesis in which the dissipation rate was equivalent to the product between the kinematic viscosity and the strain rate achieved the best description of the flow experimented by Moreau, Tanguy, Gicquel, Poirot, and Sauzin (1996).

Another important conclusion is related to the computational cost of each methodology. When an equal period of time was simulated, it was noticeable that the application of a constant characteristic length in the SEM was the methodology which required the least amount o computational time. On the other hand, the least quantity of iterations was needed when the RFG method was applied.

References

Ferziger, J. H.; Perić (2002): *Computational Methods for Fluid Dynamics*. Springer-Verlag.

Germano, M.; Piomelli, U.; Moin, P.; Cabot, W. H. (1991): A dynamic subgrid-scale eddy viscosity model. *Physics of Fluids A: Fluid Dynamics*, vol. 3, pp. 1760 – 1765.

Jarrin, N.; Benhamadouche, S.; Laurence, D.; Prosser, R. (2006): A synthetic-eddy-method for generating inflow conditions for large-eddy simulations. *International Journal of Heat and Fluid Flow*, vol. 27, pp. 585 – 593.

Kraichnan, R. H. (1970): Diffusion by a random velocity field. *Physics of Fluids*, vol. 13, pp. 22 – 31.

Lee, T.; Mateescu, D. (1998): Experimental and numerical investigation of 2-d backward-facing step flow. *Journal of Fluids and Structures*, vol. 12, pp. 703 – 716.

Lilly, D. K. (1967): The Representation of Small-Scale Turbulence in Numerical Simulation Experiments. In *IBM Scientific Computing Symposium on Environmental Sciences*, pp. 195–210, Yorktown Heights, New York, USA.

Lund, T.; Wu, X.; Squires, D. (1998): Generation of turbulent inflow data for spatially-developing boundary layer simulations. *Journal of Computational Physics*, vol. 140, pp. 233 – 258.

Mariano, F. P. (2011): *Solução Numérica das Equações de Navier-Stokes usando uma Hibridação das Metodologias Fronteira Imersa e Pseudo-Espectral de Fourier*. PhD thesis, Universidade Federal de Uberlândia, Uberlândia, Brasil, 2011.

Mariano, F. P.; Moreira, L. Q.; Silveira-Neto, A. d.; da Silva, C. B.; Pereira, J. C. F. (2010): A new incompressible navier-stokes solver combining fourier pseudo-spectral and immersed boundary method. *Computer Modeling in Engineering & Sciences*, vol. 59, pp. 181–216.

Moreau, P.; Tanguy, B.; Gicquel, P.; Poirot, M.; Sauzin, J. L. (1996): Validation expérimentale du modéle peul et du code diamant dans le cadre de l'opération a3c. *Technical Report*, vol. ONERA.

Moreira, L. Q.; Mariano, F. P.; Silveira-Neto, A. d. (2011): The importance of adequate turbulence modeling in fluid flows. *Computer Modeling in Engineering & Sciences*, vol. 75, no. 2, pp. 113 – 140.

Norris, S. E. (2001): *A Parallel Navier Stokes Solver for Natural Convection and Free Surface Flow*. PhD thesis, Faculty of Mechanical Engineering, University of Sydney, Sydney, Australia, 2001.

Pope, S. B. (2000): *Turbulent Flows*. Cambridge University Press.

Schneider, G. E.; Zedan, M. (1981): A modified strongly implicit procedure for the numerical solution of field problems. *Numerical Heat Transfer*, vol. 4, pp. 1 – 19.

Shaanan, S.; Ferziger, J. H.; Reynolds, W. C. (1975): Numerical simulation of turbulence in presence of shear. *Rep. TF-6, Dept. Mechanical Engineering, Stanford University*.

Silveira-Neto, A. d.; Grand, D.; Metais, O.; Lesieur, M. (1993): A numerical investigation of the coherent vortices in turbulence behind a backward-facing step. *Journal of Fluid Mechanics*, vol. 256, pp. 1 – 25.

Smagorinsky, J. (1963): General circulation experiments with the primitive equations. *American Metereological Society*, vol. 91, pp. 99 – 164.

Smirnov, A.; Shi, S.; Celik, I. (2001): Random flow generation technique for large eddy simulations and particle-dynamics modeling. *Journal of Fluids Engineering*, vol. 123, pp. 359 – 371.

van der Vorst, H. A. (1981): Iterative solution methods for certain sparse linear systems with a non-symmetric matrix arising from pde-problems. *Journal of Computational Physics*, vol. 44, pp. 1 – 19.

van Driest, E. R. (1956): On turbulent flow near a wall. *Journal of the Aeronautical Sciences*, vol. 23, pp. 1007 – 1011.

Vedovoto, J. M.; Silveira-Neto, A. d.; Mura, A.; Silva, L. F. F. d. (2011): Application of the method of manufactured solutions to the verification of a pressure-based finite-volume numerical scheme. *Computers & Fluids*, vol. 51, pp. 85 – 99.